Longitudinal double-spin asymmetries of inclusive jet and di-jet production at STAR

Maria Zurek[1⋆] for the STAR Collaboration

1 Argonne National Laboratory, Lemont, USA

⋆ zurek@anl.gov

Proceedings for the XXVIII International Workshop on Deep-Inelastic Scattering and Related Subjects, Stony Brook University, New York, USA, 12-16 April 2021
doi:10.21468/SciPostPhysProc.8

Abstract

The STAR experiment probes the gluon helicity distribution $\Delta g(x,Q^2)$ using collisions of longitudinally polarized protons at $\sqrt{s} = 200$ GeV and $\sqrt{s} = 510$ GeV. $\Delta g(x,Q^2)$ can be accessed through the double-spin asymmetries A_{LL} in gluon-dominated hard scattering processes via inclusive jet and dijet production. This proceedings report on recent measurements of A_{LL} for inclusive jets and dijets in the mid-pseudorapidity ($|\eta| < 1$) and dijets in the intermediate pseudrapidity ($-0.8 < \eta < 1.8$) regions. These measurements provide sensitivity to $\Delta g(x,Q^2)$ for gluon momentum fractions x from $\simeq 0.5$ down to $\simeq 0.004$. The results are in good agreement with previous STAR measurements and recent theoretical evaluations of prior world data.

Copyright M. Zurek *et al*.
This work is licensed under the Creative Commons Attribution 4.0 International License.
Published by the SciPost Foundation.

Received 30-07-2021
Accepted 06-05-2022
Published 12-07-2022
doi:10.21468/SciPostPhysProc.8.086

1 Introduction

How is the spin of the proton distributed among its quark, anti-quark, and gluon constituents? The Solenoidal Tracker at Relativistic Heavy Ion Collider (STAR) experiment is addressing this fundamental question using collisions of high-energy polarized protons.

Decades of polarized Deep Inelastic Scattering experiments shows that only about 30% of the proton's spin come from the spins of quarks and anti-quarks. The rest must originate from the the spins of the gluons and the orbital angular momenta of the quarks and gluons. Since gluon-gluon and gluon-quark scattering contributions dominate jet production at $\sqrt{s} = 200$ GeV and $\sqrt{s} = 510$ GeV at STAR, the measurements of the double-spin asymmetries of inclusive jet and dijet production in longitudinally polarized proton collisions provide sensitivity the gluon spin contribution to the proton spin.

STAR results on inclusive jet production at $\sqrt{s} = 200$ GeV and mid-pseudorapidity based on data collected in 2009 [1], when included in perturbative QCD analysis of global data, provided a strong constraint for positive gluon polarization for the momentum fraction $x > 0.05$

at a hard perturbative scale $Q^2 = 10$ GeV^2 [2, 3]. The measurements of dijet A_{LL} based on the same data [4, 5] provide more information about the initial state kinematics and further constrain the x-dependence of the gluon polarization as shown in [6]. The perturbative QCD analyses at next-to-leading order precision [2, 3] using the available world data show that gluon spins contribute approximately 40% of the total proton spin for momentum fractions $x > 0.05$ at $Q^2 = 10$ GeV^2, with a relative uncertainty of about 30%. The further reduction on the uncertainty of $\Delta g(x, Q^2)$ at $x > 0.05$ calls for measurements with improved statistics at $\sqrt{s} = 200$ GeV, while the improvements in the lower x region down to about $\simeq 0.004$ can be achieved with the measurements at higher center-of-mass energy $\sqrt{s} = 510$ GeV and more forward pseudorapidity up to $\eta \simeq 1.8$ at STAR.

In the inclusive jet and dijet A_{LL} measurements, the Time Projection Chamber [7] with a 0.5 T solenoidal magnetic field is used to reconstruct charged particle tracks in $|\eta| < 1.3$ and full range of the azimuthal angle. Barrel (BEMC) [8] and Endcap Electromagnetic Calorimeters (EEMC) [9] reconstruct the electromagnetic energy deposition in $|\eta| < 1$ and $1.1 < \eta < 2$, respectively, in full ragne of the azimuthal angle. The calorimeters are also used in jet triggers that require minimal transverse energy deposits in fixed $\Delta\eta \times \Delta\phi = 1 \times 1$ regions. Moreover, the information from Vertex Position Detectors [10] and the Zero Degree Calorimeters [11], covering $4.2 < |\eta| < 5.2$ and $|\eta| > 6.6$, respectively, is used to calculate the relative luminosities for different helicity configurations of the colliding beams.

Previously published results on inclusive jet and dijet production at $\sqrt{s} = 200$ GeV [1,4,5] are based on 2009 data corresponding to an integrated luminosity $\mathcal{L} = 20$ pb^{-1}. The results of the inclusive jet and dijet A_{LL} measurements at mid-pseudorapidity [12] presented in this proceedings are based on the most recent data collected in 2015 with an approximately twice larger figure of merit, $\mathcal{L}P^4$, corresponding to an integrated luminosity of $\mathcal{L} \simeq 52\,\text{pb}^{-1}$ and average beam polarizations for the analyzed data of $P_B \simeq 52\%$ and $P_Y \simeq 57\%$ for the RHIC "blue" (B) and "yellow" (Y) beams, respectively. The presented results at $\sqrt{s} = 510$ GeV [13] are based on the data collected in 2012 with integrated luminosity $\mathcal{L} \simeq 82$ pb^{-1} with beam polarizations of about $P_B \simeq 54\%$ and $P_Y \simeq 55\%$.

The double spin asymmetries were evaluated according to following formula:

$$A_{LL} = \frac{\sum_{\text{runs}} P_B P_Y (N^{++} - r N^{+-})}{\sum_{\text{runs}} P_B^2 P_Y^2 (N^{++} + r N^{+-})}, \tag{1}$$

where P_B and P_Y are the measured beam polarizations, N^{++} and N^{+-} are the yields of inclusive jets or dijets from colliding beam bunches with equal or opposite helicities, respectively, and r is the relative luminosity for collisions with these helicity configurations.

One of the main improvements in the data analyses of the presented results with the respect to previous STAR measurements [1, 4] is the jet-by-jet underlying-event correction. Inclusive jet p_T and dijet invariant mass, M_{inv} were corrected for underlying-event contributions using the off-axis method from [14]. The details about the event selection, jet reconstruction, and systematic effect estimation can be found in [12, 13].

2 Experiment and Data Analysis

3 Results

The inclusive jet and dijet A_{LL} versus $x_T = 2p_T/\sqrt{s}$ and $M_{inv}/\sqrt{s}$ at the parton level for $\sqrt{s} = 200$ GeV are presented in Fig. 1. The results based on STAR 2015 data [12] are shown together with the 2009 data results [1, 4] and theory evaluations from DSSV14 [2]

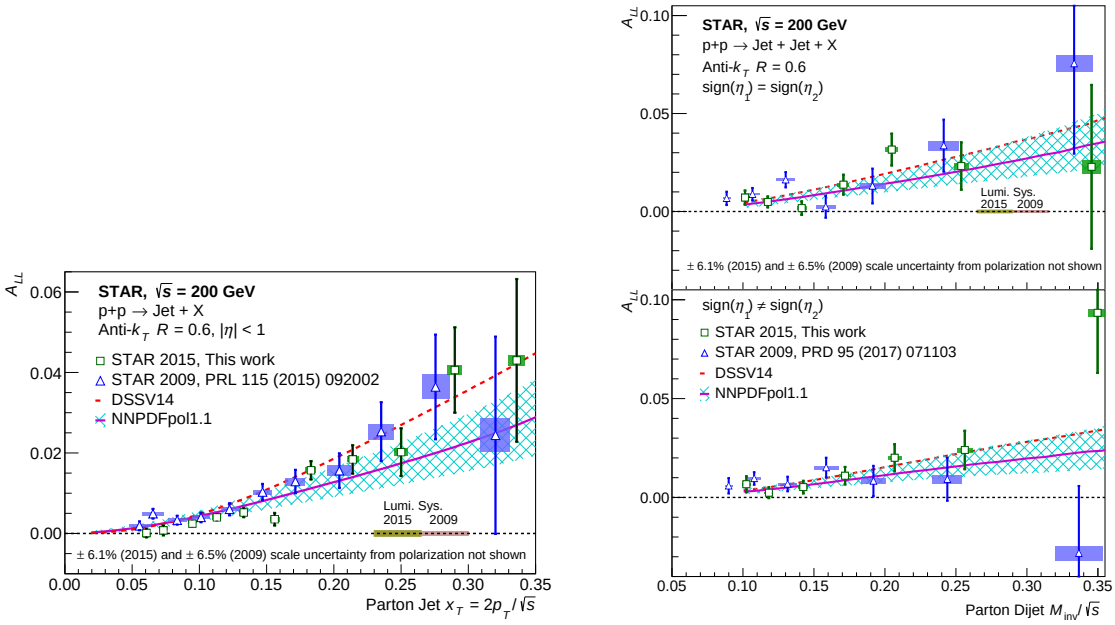

(a) (b)

Figure 1: (a) A_{LL} for inclusive jets with $|\eta| < 1.0$ versus x_T at the parton level. The square markers show the 2015 data from [12], whereas the triangle markers show the 2009 data from [1]. The error-bars show the size of the statistical uncertainties, whereas the boxes indicate the size of the systematic uncertainties. The yellow and pink bands on the horizontal axis represent the common relative luminosity uncertainty. The curves show the expected A_{LL} values for the DSSV14 [2] and NNPDFpol1.1 [3] parton distributions. (b) A_{LL} versus $M_{inv}/\sqrt{s}$ for dijets with the sign(η_1) = sign(η_2) (top) and sign$(\eta_1) \neq$ sign(η_2) (bottom) event topologies. The square markers show the 2015 data from [12], whereas the triangle markers show the 2009 data from [4]. The results are compared to theoretical predictions for dijets from DSSV14 [2] and NNPDFpol1.1 [3].

and NNPDFpol1.1 [3]. The inclusive jet A_{LL} is presented for the pseudorapidity region of $|\eta| < 1$, while the dijet A_{LL} is shown for two different event topologies, sign(η_1) = sign(η_2) and sign$(\eta_1) \neq$ sign(η_2), where 1 and 2 denotes the two jets. The different topologies sample different regions of x. The same-sign events probe more asymmetric collisions with better separated the high-x and low-x distributions, while the opposite-sign events probes an intermediate-x range (see, e.g., Fig. 3 in Ref. [4]).

Figure 2 presents the first results from STAR for inclusive jet A_{LL} at $\sqrt{s} = 510$ GeV versus $x_T = 2p_T/\sqrt{s}$ from 2012 STAR data [13] in the mid-pseudorapidity region ($|\eta| < 0.9$) compared with the measurements at $\sqrt{s} = 200$ GeV from [1]. Figure 3 shows dijet A_{LL} versus M_{inv} at the parton level for the same dataset. The preliminary results for the measurement at the intermediate pseudorapidity ($-0.8 < \eta < 1.8$) are shown in Fig. 3a, whereas Fig. 3b shows results from the mid-pseudorapidity region from [13]. The curves representing theoretical evaluations of A_{LL} for DSSV14 [2] and NNPDFpol1.1 [3] parton distributions are also presented. The dijet results are divided into different event topologies probing different x regions, similarly to the $\sqrt{s} = 200$ GeV results. The intermediate rapidity preliminary results are divided into three classes based on the pseudorapidities of the jets in the dijet pair: one jet in the east half of the BEMC ($-0.8 < \eta < 0$) or the west half of the BEMC ($0 < \eta < 0.8$) and the other jet in the EEMC ($0.8 < \eta < 1.8$), or both jets in the EEMC. The last category

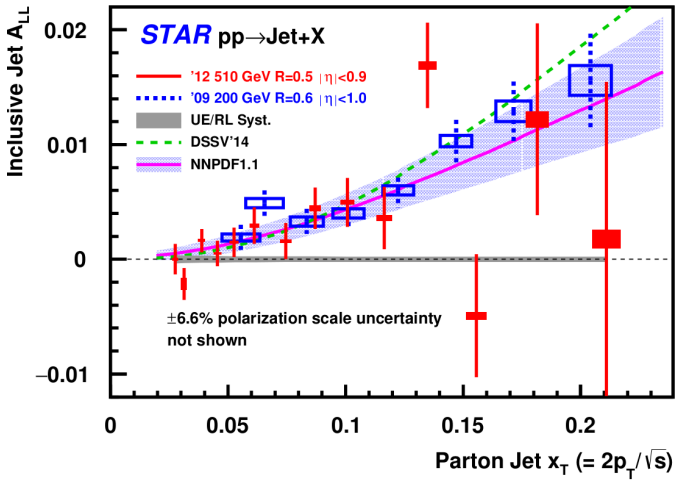

Figure 2: A_{LL} for inclusive jets with $|\eta| < 0.9$ versus x_T at the parton level. The filled red markers show the 2012 data at 510 GeV from [13], whereas the open blue markers show the 2009 data at 200 GeV from [1]. The error-bars show the size of the statistical uncertainties, whereas the boxes indicate the size of the systematic uncertainties. The gray band on the horizontal axis represent the common relative luminosity uncertainty. The curves show the expected A_{LL} values for the DSSV14 [2] and NNPDFpol1.1 [3] parton distributions.

probes the most asymmetric collisions with separated the high-x and low-x distributions down to $\simeq 0.004$ however with large statistical uncertainties of the obtained results. For the mid-pseudorapidity results, the individual jets in the dijet were sorted into the following three categories: forward ($0.3 < \eta < 0.9$), central ($|\eta| < 0.3$), and backward ($-0.9 < \eta < -0.3$). The final A_{LL} results are presented for four dijet event topologies, namely, with forward-forward jets, forward-central jets, central-central jets and forward-backward jets. The forward-forward and forward-central configurations probe the most asymmetric collisions with low-x down to $x \simeq 0.015$. The forward-forward and central-central events probes collisions with $|\cos\theta^*|$ near zero, whereas forward-central and forward-backward events are more sensitive to larger $|\cos\theta^*|$, where θ^* is the scattering angle in the center-of-mass frame of scattering partons.

4 Conclusions and Outlook

STAR has achieved unique insights into the helicity structure of the proton, through the study of the longitudinal double-spin asymmetries in the production cross sections of inclusive jet and dijet probes sensitive to $\Delta g(x, Q^2)$. STAR inclusive jet results [1] provided first evidence for a positive polarization of the gluons in the polarized proton for $x > 0.05$ upon their inclusion in global analyses. The presented in this proceedings results based on data collected in 2015 and 2012 are in good agreement with the prior STAR measurements as well as the theoretical evaluations from DSSV14 [2] and NNPDFpol1.1 [3] that include the prior inclusive jet data [1]. The 2015 results with approximately twice larger figure of merit and with improved systematic uncertainties with respect to the prior data at $\sqrt{s} = 200$ GeV will provide important constraints on the magnitude and shape of the gluon helicity distribution for $x > 0.05$ when included in the future global analyses of the polarized parton distribution functions. The first results at 510 GeV at mid-pseudorapidity and preliminary results at intermediate pseudorapidity will provide further constraints, especially in the region $x < 0.05$ unconstrained by any data in

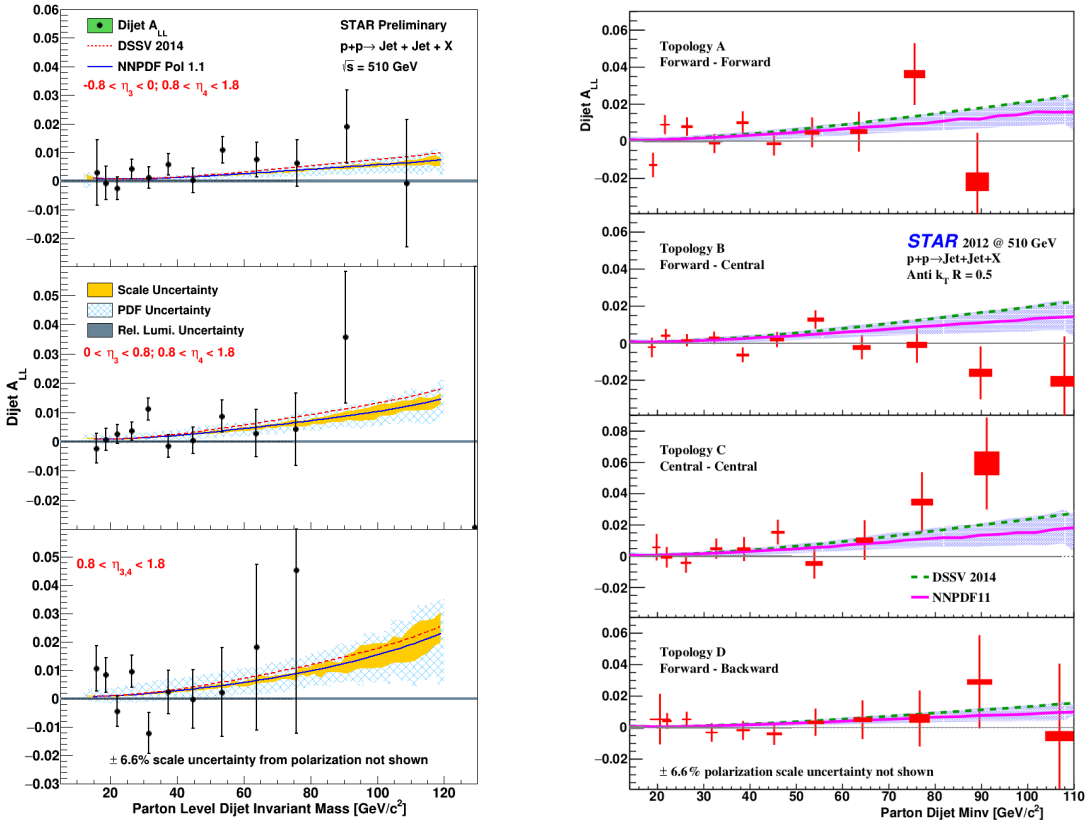

(a) (b)

Figure 3: A_{LL} as a function of parton-level invariant mass for dijets from 2012 STAR data at 510 GeV. Figure (a) presents the preliminary results obtained for the East Barrel-Endcap (top), West Barrel-Endcap (middle) and Endcap-Endcap (bottom) event topologies with statistical uncertainties only. Figure (b) presents results from [13] for different event topologies in Barrel calorimeter as described in the text. The error-bars show the size of the statistical uncertainties, whereas the boxes indicate the size of the systematic uncertainties. The curves represent theoretical evaluations of A_{LL} for DSSV14 [2] and NNPDFpol1.1 [3] parton distributions.

the prior global analyses. Further precision at low-x region from STAR will be possible with the measurements based on data collected at 510 GeV in 2013 with the integrated luminosity $\mathcal{L} \simeq 250$ pb^{-1} and 2015 data in more forward rapidity region of EEMC. Since Relativistic Heavy Ion Collider concluded the data taking with longitudinally polarized protons in 2015, the STAR data are anticipated to provide the most precise insights in $\Delta g(x, Q^2)$ well into the future.

Acknowledgements

We thank the RHIC Operations Group and RCF at BNL. This work is supported by U.S. DOE Office of Science.

References

[1] L. Adamczyk et al., *Precision Measurement of the Longitudinal Double-spin Asymmetry for Inclusive Jet Production in Polarized Proton Collisions at* $\sqrt{s} = 200$ *GeV*, Phys. Rev. Lett. **115**, 092002 (2015), doi:10.1103/PhysRevLett.115.092002.

[2] D. de Florian, R. Sassot, M. Stratmann and W. Vogelsang, *Evidence for Polarization of Gluons in the Proton*, Phys. Rev. Lett. **113**, 012001 (2014), doi:10.1103/PhysRevLett.113.012001.

[3] E. R. Nocera, R. D. Ball, S. Forte, G. Ridolfi and J. Rojo, *A first unbiased global determination of polarized PDFs and their uncertainties*, Nucl. Phys. B **887**, 276 (2014), doi:10.1016/j.nuclphysb.2014.08.008.

[4] L. Adamczyk et al., *Measurement of the cross section and longitudinal double-spin asymmetry for di-jet production in polarized pp collisions at* $\sqrt{s} = 200$ *GeV*, Phys. Rev. D **95**, 071103 (2017), doi:10.1103/PhysRevD.95.071103.

[5] J. Adam et al., *Longitudinal double-spin asymmetries for dijet production at intermediate pseudorapidity in polarized pp collisions at* $\sqrt{s} = 200$ *GeV*, Phys. Rev. D **98**, 032011 (2018), doi:10.1103/PhysRevD.98.032011.

[6] D. de Florian, G. Agustín Lucero, R. Sassot, M. Stratmann and W. Vogelsang, *Monte Carlo sampling variant of the DSSV14 set of helicity parton densities*, Phys. Rev. D **100**, 114027 (2019), doi:10.1103/PhysRevD.100.114027.

[7] M. Anderson et al., *The STAR time projection chamber: a unique tool for studying high multiplicity events at RHIC*, Nucl. Instrum. Meth. A **499**, 659 (2003), doi:10.1016/S0168-9002(02)01964-2.

[8] M. Beddo et al., *The STAR Barrel Electromagnetic Calorimeter*, Nucl. Instrum. Meth. A **499**, 725 (2003), doi:10.1016/S0168-9002(02)01970-8.

[9] C. E. Allgower et al., *The STAR endcap electromagnetic calorimeter*, Nucl. Instrum. Meth. A **499**, 740 (2003), doi:10.1016/S0168-9002(02)01971-X.

[10] W. J. Llope et al., *The STAR Vertex Position Detector*, Nucl. Instrum. Meth. A **759**, 23 (2014), doi:10.1016/j.nima.2014.04.080.

[11] C. Adler, A. Denisov, E. Garcia, M. Murray, H. Stroebele and S. White, *The RHIC zero degree calorimeters*, Nucl. Instrum. Meth. A **470**, 488 (2001), doi:10.1016/S0168-9002(01)00627-1.

[12] M. Abdallah et al., *Longitudinal double-spin asymmetry for inclusive jet and dijet production in polarized proton collisions at* $\sqrt{s} = 200$ *GeV*, Phys. Rev. D **103**, L091103 (2021), doi:10.1103/PhysRevD.103.L091103.

[13] J. Adam et al., *Longitudinal double-spin asymmetry for inclusive jet and dijet production in pp collisions at* $\sqrt{s} = 510$ *GeV*, Phys. Rev. D **100**, 052005 (2019), doi:10.1103/PhysRevD.100.052005.

[14] B. B. Abelev et al., *Charged jet cross sections and properties in proton-proton collisions at* $\sqrt{s} = 7$ *TeV*, Phys. Rev. D **91**, 112012 (2015), doi:10.1103/PhysRevD.91.112012.